JOURNAL OF TISSUE ENGINEERING AND REGENERATIVE MEDICINE
J Tissue Eng Regen Med (2015)
Published online in Wiley Online Library (wileyonlinelibrary.com) **DOI:** 10.1002/term.2079

RESEARCH ARTICLE

Ultrasound-guided plasma rich in growth factors injections and scaffolds hasten motor nerve functional recovery in an ovine model of nerve crush injury

Mikel Sánchez[1,2]*, E. Anitua[3], D. Delgado[2], R. Prado[4], P. Sánchez[2], N. Fiz[1], J. Guadilla[1], J. Azofra[1], O. Pompei[1], G. Orive[3], M. Ortega[5], T. Yoshioka[6] and S. Padilla[4]
[1]*Arthroscopic Surgery Unit, Hospital Vithas San Jose, Vitoria-Gasteiz, Spain*
[2]*Arthroscopic Surgery Unit Research, Hospital Vithas San Jose, Vitoria-Gasteiz, Spain*
[3]*Eduardo Anitua Foundation for Biomedical Research, Vitoria-Gasteiz, Spain*
[4]*Biotechnology Institute (BTI), Vitoria-Gasteiz, Spain*
[5]*Clinical Neurophysiology Unit, Galdakao-Usánsolo Hospital, Bilbao, Spain*
[6]*Division of Regenerative Medicine for Musculoskeletal System, Department of Orthopaedic Surgery, University of Tsukuba, Japan*

Abstract

In the present study we evaluated the motor recovery process of peripheral nerve injury (PNI), based on electrophysiological and histomorphometric criteria, after treatment with plasma rich in growth factors (PRGF) injections and scaffolds in an ovine model. Three groups of sheep underwent a nerve crush lesion: the first group ($n = 3$) was left to recover spontaneously (SR); the second group was administered saline injections (SI; $n = 5$) and a third group ($n = 6$) received PRGF injections and scaffolds immediately after the crush injury. At post-intervention week 8, 70% of sheep in the PRGF group were CMAP-positive, with no electrophysiological response in the rest of the groups. Histomorphometric analysis 12 weeks after the surgical intervention revealed that the average axonal density of the SR (1184 ± 864 axons/μm^2) and SI (3109 ± 2450 axons/μm^2) groups was significantly inferior to the control (8427 ± 2433 axons/μm^2) and also inferior to the PRGF group (5276 ± 4148 axons/μm^2), showing no significant differences between the control and PRGF groups. The axonal size of the SR and SI groups was significantly smaller compared with the control group (18 ± 4 μm^2), whereas the axonal size of the PRGF group (6 ± 5 μm^2) did not show statistical differences from the control. Morphometry of the target muscles indicated that the PRGF group had the lowest percentage volume reduction 12 weeks after the crush injury. The PRGF group had larger muscle fibre areas than the SI and SR groups, although the differences did not reach statistical significance. Overall, these data suggest that the PRGF injections and scaffolds hastened functional axon recovery and dampened atrophy of the target muscles in an ovine model.

Received 10 February 2015; Revised 18 June 2015; Accepted 23 June 2015

Keywords **PRGF; platelet-rich plasma; growth factors; peripheral nerve injury; muscle atrophy; fibrin; scaffold; compound muscle action potential**

1. Introduction

In mammals, axons of injured peripheral nerves (PNI) whose damage was brought about by a crush mechanism can and do regenerate, but often the outcomes of functional recovery are incomplete or suboptimal (Allodi *et al*., 2012; Höke, 2006). Despite the substantial contribution made by microsurgical treatment methods still on hand for nerve repair, the treatment of PNI remains a challenging surgical, clinical and biological task (Kuffler, 2014). In recent years attention has turned to *in vivo* tissue-engineering approaches through molecular

*Correspondence to: Mikel Sanchez, Arthroscopic Surgery Unit, Hospital Vithas San Jose, C/ Beato Tomás de Zumarraga 10, 01008 Vitoria, Spain. E-mail: mikel.sanchez@ucatrauma.com

interventions, and these are offering the most promising results in this field (Daly *et al*., 2013; Deumens *et al*., 2010).

There is a growing body of evidence indicating that platelet-rich plasma (PRP) (Emel *et al*., 2011; Farrag *et al*., 2007; Sanchez *et al*., 2014; Sariguney *et al*., 2008; Takeuchi *et al*., 2012; Wu *et al*., 2012; Ye *et al*., 2012; Zheng *et al*., 2014), fibrin (Akassoglou *et al*., 2003; Chernousov and Carey, 2003; Lee *et al*., 2003; Sakiyama-Elbert and Hubbell, 2000; Wood *et al*., 2009; Zheng *et al*., 2014) and growth factors (GFs) (Cheng and Feldman, 1997; de Boer *et al*., 2012; Emel *et al*., 2011; Hobson *et al*., 2000; Hoke *et al*., 2001; Ikeda *et al*., 2014; Jungnickel *et al*., 2006; Lee *et al*., 2003; Luo *et al*., 2012; Mohammadi *et al*., 2013; Rosner *et al*., 2005; Sakiyama-Elbert and Hubbell, 2000; Tang *et al*., 2013; Yin *et al*., 2001) play an important role in the axon regeneration that follows peripheral nerve trauma and damage to neuromuscular junctions (Borselli *et al*., 2010), and in neuron survival (Anitua *et al*., 2013; Currie *et al*., 2009). PRP injections and scaffolds are part of an innovative biological therapeutic strategy to locally and gradually provide the injured tissue with GFs that have previously been sequestered within the biodegradable fibrin matrix (Anitua *et al*., 2015; Martino *et al*., 2013) and which might prompt and enhance axonal regeneration (Lee *et al*., 2003; Sakiyama-Elbert and Hubbell, 2000; Wood *et al*., 2009). Growth factors such as IGF1 (Cheng and Feldman, 1997; Emel *et al*., 2011; Mohammadi *et al*., 2013), BDNF, TGFβ1(Luo *et al*., 2012; Rosner *et al*., 2005), FGF (Ikeda *et al*., 2014; Jungnickel *et al*., 2006), VEGF (Hobson *et al*., 2000; Hoke *et al*., 2001) and NGF (de Boer *et al*., 2012; Lee *et al*., 2003; Sakiyama-Elbert and Hubbell, 2000; Tang *et al*., 2013; Yin *et al*., 2001) are powerful bioactive mediators in tissue regeneration (Anitua *et al*., 2010; Nurden *et al*., 2008) and have been shown to act as enhancers of axonal sprouting. Fibrin matrix and the GFs within it fulfil two vital criteria: first, to produce a prolonged and gradual delivery system of growth–survival–chemotaxis and anti-inflammatory supporting cues; and second, to function as a transient nerve-guidance scaffold for axonal sprouting (Anitua *et al*., 2012; Deumens *et al*., 2010; Eccleston *et al*., 1993; Farrag *et al*., 2007; Kuffler, 2014; Wood *et al*., 2009). In doing so, a plasma rich in growth factors (PRGF) therapeutic approach might allow the sprouting of growth cones and promote the survival, proliferation and differentiation of Schwann cells (SCs), which synthesize and release neurotrophic factors. This therapy may additionally avoid, or at least diminish, undesirable consequences such as fibrotic scars, and thereby lead to functional recovery of the nerve–muscle unit (Sanchez *et al*., 2014; Sariguney *et al*., 2008; Takeuchi *et al*., 2012; Wu *et al*., 2012; Ye *et al*., 2012). Evaluation of the motor recovery process of peripheral nerve injury was based on electrophysiological and histomorphometric criteria 4, 8 and 12 weeks after the peripheral nerve injuries were treated with surgical and molecular intervention (Farrag *et al*., 2007; Sariguney *et al*., 2008; Wang *et al*., 2008).

The aim of our study was to assess whether the application of PRGF, a leukocyte-free PRP, in the form of injections and scaffolds, could improve the intrinsic ability of neurons to regenerate and speed up functional axonal recovery.

2. Materials and methods

2.1. Animals

In this study, 16 healthy, skeletally mature Latxa sheep (*Ovis aries*, Latxa breed) were used. Their body condition score was assessed by a senior veterinarian, by estimating muscle and fat deposition over and around the vertebrae in the loin region (for further details, see supporting information, Table S1). Animal handling and surgical procedures were carried out according to the directive of the European Parliament and Council of the European Communities (2010/63/UE) and the Spanish legislation (RD 1201/2005 and Law 32/2007). The protocol of this study was approved by the ethics committee of the Provincial Government of Álava (DFA), Spain. Animals were fed grass silage *ad libitum* and 0.5 kg corn silage/sheep; access to drinking water was permanent. The sheep were divided into three different groups (Figure 1A), maintaining a homogeneous medium weight between groups: PRGF group (PRGF scaffold + infiltrations; $n = 6$); saline group (SI; saline infiltrations, $n = 6$) and spontaneous recovery (SR) group (no treatment, $n = 4$).

2.2. Experimental common peroneal nerve injury model

The sheep were fasted for 48 h before surgery, and drinking water was suppressed 24 h before intervention to avoid complications during the process. The animals were anaesthetized with an intramuscular combination of xylazine (0.08 mg/kg) and ketamine hydrochloride (5 mg/kg).

The left limb of the sheep's gluteal region was shaved and swabbed with povidone–iodine solution. Using aseptic technique, the common peroneal nerve (CPN) above the bifurcation point of its peroneal and tibial branch division was exposed by a 3 cm longitudinal incision through the skin at the level of the proximal site of the fibular head, and dissected through a gluteal muscle-splitting approach. Careful blunt dissection with atraumatic technique was performed to isolate the CPN from the surrounding connective tissue over a length of 2–2.5 cm (Figure 2A). A Kocher forceps was used to perform CPN compression injuries (Figure 2B); 11 kg compression pressure (data not shown) was applied (second position of Kocher) and the ends of the Kocher forceps were protected to avoid sectioning nerve structures. The compression was released after 7 min (Figure 2C) and the wounds were closed in layers with a 3-0 Ethicon silk suture. The

DOI: 10.1002/term

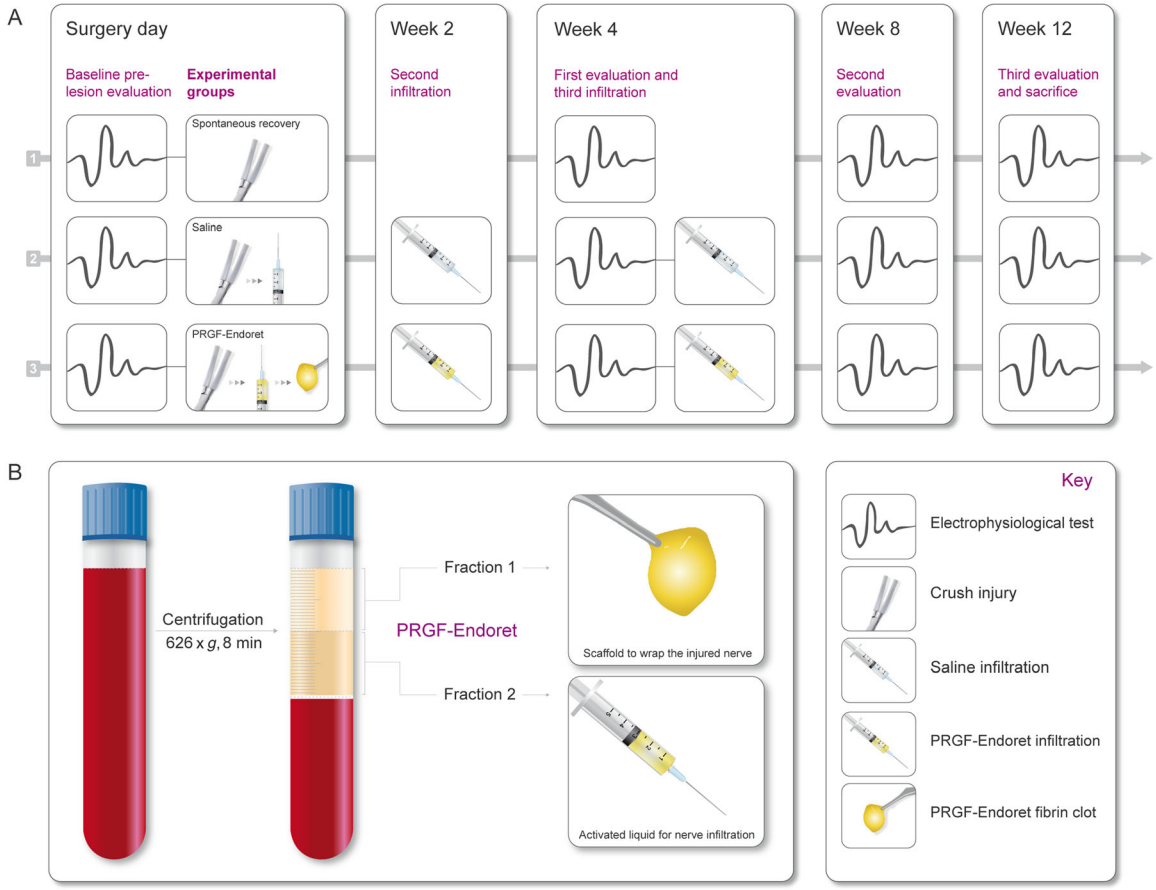

Figure 1. Experimental design and PRGF protocol for nerve regeneration. (A) Schematic illustration of the experimental design, including the three experimental groups as well as the treatments and evaluations conducted during the course of the study. (B) Summary of PRGF preparation and intended use of each of the fractions: F1 to wrap the injured nerve; F2 to be injected peri- and intraneurally and thus act as an *in situ* gelling scaffold

resulting injury was an axonotmesis at grade II, preserving the continuity of the perineurium (Lundborg, 2004).

After recovery from anaesthesia the animals were housed for 10 days in order to monitor and maintain analgesic and antibiotic therapy. After removing the staples 10 days after surgery, the animals were incorporated into the overall herd. Intramuscular Flumixin Meglubine every 8 h for three days after surgery was used as analgesia. Antibiotic treatment was based on Cefonicid (1 g) daily for 5 days.

2.3. PRGF preparation and characterization

For PRGF preparation, a total of 40 ml peripheral venous blood was withdrawn into 5 ml tubes containing 3.8% w/v sodium citrate. Blood was centrifuged for 8 min at $626 \times g$ at room temperature in a PRGF System II (BTI Biotechnology Institute, Vitoria-Gasteiz, Spain). After centrifugation, three layers were obtained, plasma, buffy coat and packed red blood cells. The upper 1–1.5 ml plasma was collected in order to prepare PRGF scaffolds/membranes; this poor-platelet fraction (F1) contains a number of platelets similar to that in peripheral blood. The next layer corresponds to 1 ml platelet-rich plasma fraction (F2), with an increased concentration of platelets compared with peripheral blood. F2 was collected avoiding the leukocyte layer, and was used to perform intraneural infiltrations (Figure 1B). The protocol for obtaining PRGF in sheep is an adaptation of the protocol for humans previously described (Anitua *et al.*, 2012). The number of erythrocytes, leukocytes and platelets from whole blood, F1 and F2, were assessed using the Horiba Micros VET ABC (Horiba ABX, Montpellier, France). For each formulation, the platelet enrichment factor (Anitua *et al.*, 2012) and platelet:leukocyte ratio were also calculated (Boswell *et al.*, 2014).

2.4. Treatment administration

Infiltrations were performed under anaesthesia using intramuscular ketamine hydrochloride (5 mg/kg). Both the PRGF and saline groups were infiltrated with three intraneural injections of PRGF and saline, respectively; the interval between each infiltration was 2 weeks. Concerning PRGF infiltrations, F2 was activated in a controlled way by the addition of $CaCl_2$ (10%), just before injection (50 µl $CaCl_2$/ml PRGF).

The first infiltration was performed immediately after causing the injury, injecting 3 ml PRGF (activated F2) or saline, depending on the group, by means of a 25G needle

DOI: 10.1002/term

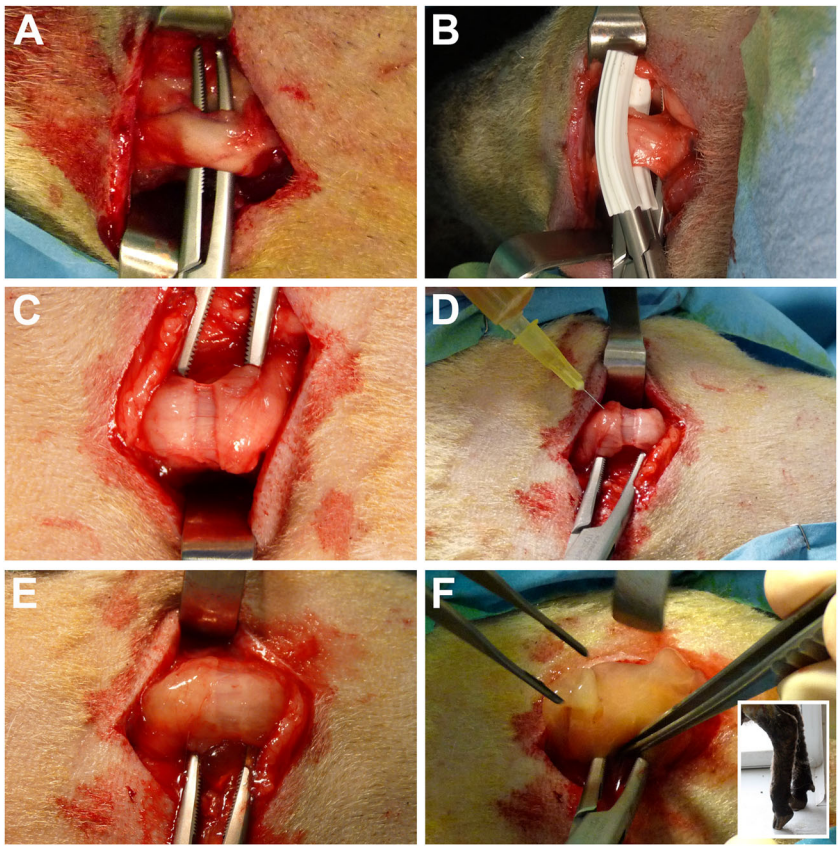

Figure 2. Animal model and surgical procedures. First, (A) the common peroneal nerve was isolated from the surrounding connective tissue and (B) compression with Kocher forceps was applied for 7 min. (C) Image of the injured nerve. (D) PRGF infiltration in injured nerve. (E) Note that the nerve has swollen with the infiltration. (F) Finally, a PRGF scaffold is applied, wrapping the injury; (insert) the clinical outcome of the injury is appreciated, with the bent leg without the possibility of total support on the ground

at the site of compression, proximal and distal to the lesion (Figure 2D, E). Furthermore, in the case of the PRGF group, a PRGF membrane was placed around the nerve lesion (Figure 2F). It was elaborated with 4 ml F1, which was activated with 200 µl $CaCl_2$ (10%) and maintained for 15 min at room temperature until the formation of a membrane.

Second and third intraneural injections (SI and PRGF groups) were carried out by ultrasound guidance (Figure 3A) at weeks 2 and 4, respectively. An 8.0–13.0 MHz multi-frequency linear probe (12L-SC, Venue 40 Musculoskeletal, GE Healthcare) was used. Ultrasound examination was performed by an experienced radiologist before each injection. Diagnosis of the injured site was based on the continuity, echogenicity and thickness of the common peroneal nerve (Figure 3B). First, the probe was aligned repeatedly with the long and short axes of the common peroneal nerve. Once the lesion was located, the injection was performed using a 22-gauge needle (25 mm) just below the probe to allow visualization of the needle and ensure intraneural and perineural infiltration of PRGF or saline; 3 ml PRGF (activated F2) or saline was gently and slowly injected within the epineurium and also around the common peroneal nerve, changing the entry point of the needle along the lesion. Details of the structures and the infiltration process are provided in Figure 3C (see also supporting information, Video S1).

2.5. Electrophysiological studies

We studied the left peroneal nerve in all animals. Baseline registration was performed before the injury and later serial controls were conducted 4, 8 and 12 weeks after the insult. A portable electromyograph of two-channel Alpine Keypoint (Alpine Biomed Aps, Skovlunde, Denmark) was used, with a monopolar needle for stimulation electrodes and a concentric needle for the record.

In neurographic and electromyographic studies, motor latency was evaluated from the head of the fibula to the peroneus tertius muscle, as well as the compound motor action potential (CMAP) amplitude and the morphology of the response. Moreover, the presence or absence of acute signs of denervation and re-innervation was noted in the left anterior peroneus tertius muscle in every control.

2.6. Sacrifice and macroscopic muscle atrophy evaluation

After the final evaluation at the third month, the sacrifice of animals was performed humanely, using intravenous T-61 (MSD Animal Health, Salamanca, Spain) as euthanasia. The peroneus tertius and peroneus longus muscles were removed from both legs. Atrophy of these muscles was evaluated macroscopically as well as histologically.

DOI: 10.1002/term

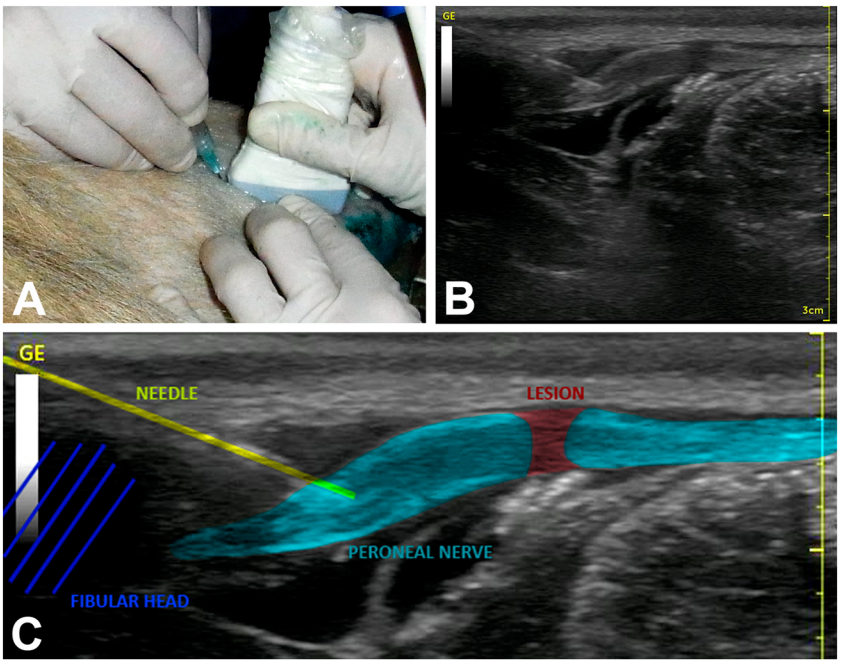

Figure 3. Ultrasound-guided infiltrations. (A) Photograph showing an ultrasound-guided infiltration. (B) Ultrasound image during the infiltration procedure. (C) Detail of anatomical structures during infiltration. See also an ultrasound-guided infiltration video (see supporting information, Video S1)

Macroscopic assessment was conducted by weighing muscles and comparing the weights of the injured leg with those of the healthy leg. The same comparison was also performed for the peroneus tertius muscle by volumetric analysis, using a cone beam technique (Galileos 3D Imaging System, Bensheim, Germany). The obtained DICOM images were analysed using BTI scan II software v. II (BTI Biotechnology Institute, Vitoria-Gasteiz, Spain).

2.7. Histological and histomorphometric assessment

The nerves were dissected and fixed in 4% paraformaldehyde for at least 24 h. The muscles were treated similarly after the macroscopic analysis. Later, all samples were dehydrated in an increasing series of graded alcohols, rinsed in xylene substitute and embedded in paraffin. The obtained blocks were cut transversely at 3.5 μm thickness and the resulting sections were stained with haematoxylin and eosin (H&E).

For nerve and muscle histomorphometric analysis, the samples were examined by conventional optical microscopy, using a Leica DMLB microscope, and photographed with a digital camera (Leica DFC 300 FX, Leica Microsystems, Wetzlar, Germany). The images were analysed manually and/or semi-automatically using ImageJ software v. 1.4 (NIH, Bethesda, MD, USA).

Anti-mouse monoclonal antibody (clone RNF405) to 200 kDa neurofilament heavy polypeptide (reactive in sheep tissue) was used to detect axons in nerve samples. The immunohistochemical reaction was developed by Vector VIP Substrate (Vector Laboratories, Burlingame, USA), generating a dark purple reaction product in the presence of horseradish peroxidase (HRP) enzyme. The axonal size (μm^2) and density (number of axons/μm^2) was quantified in three random fields at ×40 magnification.

The size of myofibres was determined by analysis of the cross-sectional area (CSA), measuring the minimal Feret's diameter, defined as the closest possible distance of two parallel tangents at opposing borders of the muscle fibre. This parameter was chosen to minimize variability due to the orientation of the muscle sample (Briguet *et al.*, 2004). For each sample, at least three random fields at ×40 (up to 0.92 mm^2) were evaluated in samples stained with picrosirius red (Polysciences, Warrington, USA).

2.8. Statistical analysis

Statistical analysis was performed using PASW Statistics 18.0 (SPSS®, Chicago, IL, USA). Normal distribution of samples was assessed by the Shapiro–Wilk test and homogeneity of variance by the Levene test. The different treatments were compared by analysis of varience (ANOVA). In case the data did not fit the normal distribution or the variances were not homogeneous, the non-parametric Kruskal–Wallis one-way ANOVA was applied. Differences between groups were considered statistically significant at $p < 0.05$.

3. Results

3.1. Animal model and features of experimental groups

The values of the main physical features of the three groups showed no significant differences among groups

DOI: 10.1002/term

(see supporting information, Table S1). During the follow-up period, two sheep (one from the spontaneous recovery group and one from the saline group) died and were thus excluded from the study.

3.2. Characterization of the PRGF

The scientific rationale behind the biological effects of PRGF is based on the composition of platelets and the release of their growth factors, and on fibrin where GFs were sequestered. The average enrichment in platelets for F1 and F2 was 0.8 ± 0.2 and 1.4 ± 0.5, respectively (Table 1). Both PRGF fractions had only a residual amount of leukocytes and erythrocytes, being classified as pure PRPs (P-PRP). In addition, we calculated the platelet:leukocyte ratio for the whole blood, F1 and F2, whose values were 59 ± 25, 1686 ± 1090 and 2562 ± 1723, respectively (Table 1).

3.3. Electrophysiological parameters assessment

The first electrophysiological evaluation, 4 weeks after the surgical and molecular intervention, showed in all groups a drop from their physiological baseline values to a flat line, with no signs of physiological response and an absence of CMAP (Figure 4). At the post-intervention week 8, stimulation of the proximal common peroneal nerve elicited a positive electrophysiological response, with a reliable though low amplitude and prolonged onset latency CMAP only in the PRGF treated group, where 70% of sheep within the group were responders (Figure 4A). However, 12 weeks after surgical intervention the CMAP returned to the rest of the groups, although with a delayed onset latency and a low amplitude. No statistically significant differences were determined among the groups for these parameters (Figure 4). Nevertheless, the mean median CMAP latency and CMAP amplitude 12 weeks after the surgical intervention were longer and lower, respectively, than that of baseline in all groups (Figure 4B, C). At post-intervention week 12, the three groups reached the same percentage of improvement related to the initial electrophysiological values (CMAP baseline), but notably the PRGF treated group had already shown this improvement at week 8 (Figure 4D).

3.4. Axonal histomorphometric analysis

Histological analysis of transversal sections of the regenerated nerve tissues revealed differences in nerve architecture among the treated groups, with a better arrangement of axons in the PRGF-treated group, whereas the SI and SR groups had more random, asymmetrical spacing of fibres. The analysis indicated that, although there exists spontaneous nerve

Table 1. PRGF characterization

	Leukocytes ($\times 10^3/\mu l$)	Erythrocytes ($\times 10^6/\mu l$)	Platelets ($\times 10^3/\mu l$)	Platelet:leukocyte ratio	Platelet enrichment
Whole blood	4.73 ± 1.24	10.19 ± 1.40	256 ± 51	59 ± 24	1.0 ± 0.0
PRGF-F_1	0.20 ± 0.18	0.01 ± 0.00	202 ± 80	1686 ± 1090	0.8 ± 0.2
PRGF-F_2	0.16 ± 0.09	0.01 ± 0.00	349 ± 179	2562 ± 1723	1.4 ± 0.5

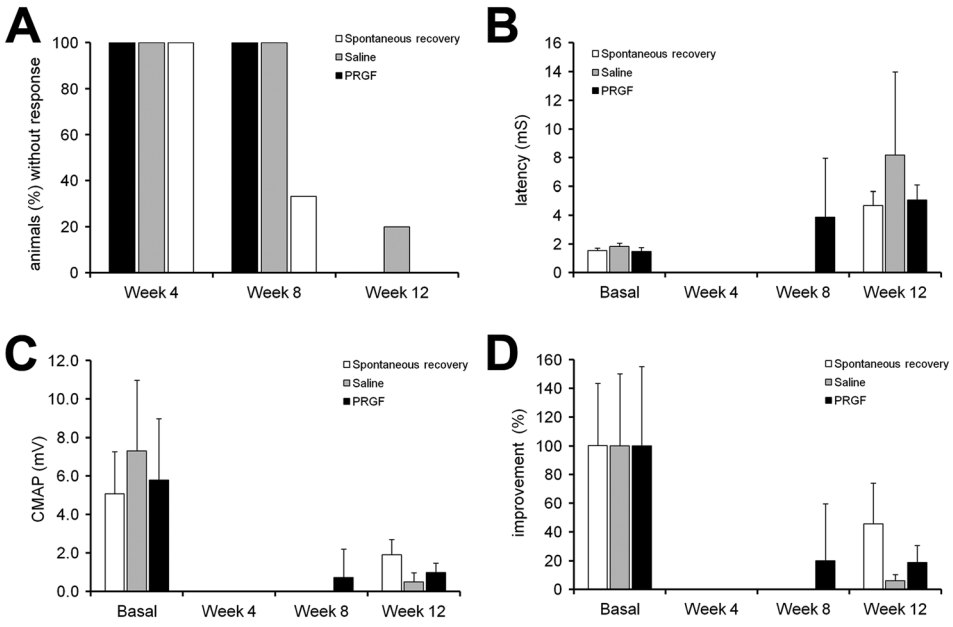

Figure 4. Electrophysiological study. (A) Percentage of animals without electrophysiological response. (B) Chart showing the values of signal latency (mS). (C) Compound motor action potential (CMAP) values (mV). (D) Percentage of improvement related to the initial CMAP baseline

DOI: 10.1002/term

regeneration, the surgical intervention with either saline or PRGF improved it, but the PRGF group was clearly the one with better regeneration (Figure 5A). Immunostaining for neurofilaments displayed a thicker axonal density and an increased number of positively stained neurofilaments in the PRGF-treated group compared with other groups.

Histomorphometric analysis of the common peroneal nerve biopsies taken at the crush area 12 weeks after the surgical intervention revealed that the average axonal density, which is a measure of the quality of the regenerating nerve, in the spontaneous recovery (1184 ± 864 axons/μm^2) and saline (3109 ± 2450 axons/μm^2) groups was inferior ($p < 0.05$) to that of the control (8427 ± 2433 axons/μm^2) and inferior to that of the PRGF group (5276 ± 4148 axons/μm^2). However, the differences between the control and PRGF groups were not significant, thus demonstrating an axonal density in the PRGF group similar to that in the non-injured contralateral nerves (Figure 5B). Axonal size was assessed as a parameter of the maturity of the regenerating nerve fibres. The SR and SI groups contained significantly ($p < 0.05$) smaller nerve fibres compared to the control group ($18 \pm 4\,\mu m^2$), whereas the axonal size of the PRGF group ($6 \pm 5\,\mu m^2$) did not show statistical differences from the control (Figure 5C).

3.5. Examination of tibialis and extensores muscles

The morphometry of target muscles (peroneous tertius and peroneus longus) indicated a different degree of atrophy among groups, with the PRGF group displaying the lowest percentage weight (Figure 6A, B) and volume (Figure 6C) reductions 12 weeks after the crush injury; however, the differences did not reach statistical significance. The functional state of the target muscles was assessed by evaluation of the cross-sectional area of muscle fibres. The PRGF group showed a CSA pattern more similar to that of the control group than the to other injured group (Figure 7A). The PRGF group had larger muscle fibre CSA (minimal Feret's diameter) than the SI or SR groups, although the differences did not reach statistical significance in either the peroneous tertius (Figure 7C) or the peroneus longus (Figure 7C). The macroscopic and histological muscle assessment suggested an attenuation of target muscle atrophy in the PRGF-treated group.

4. Discussion

The decision to carry out a study on sheep and select a crush nerve injury hinged on the fact that long-distance regeneration (Höke, 2006; Luo *et al*., 2012) and crush injuries are more appropriate to investigate the intrinsic cellular and molecular events taking place in peripheral nerve injuries, and to assess whether these molecular interventions might speed up axon regeneration and, consequently, to further gauge the effectiveness of reinnervation (Rodríguez *et al*., 2004). The results of the present study showed that PRGF injections and scaffolds enhance peripheral nerve regeneration by improving axonal sprouting and myelination of newly generated axons, a result which correlated with an early positive electrophysiological response at week 8 after the PRGF molecular intervention as a sign of functional recovery. In addition, this earlier positive electrophysiological response shown by the PRGF group, compared with the spontaneous recovery and saline groups, might account

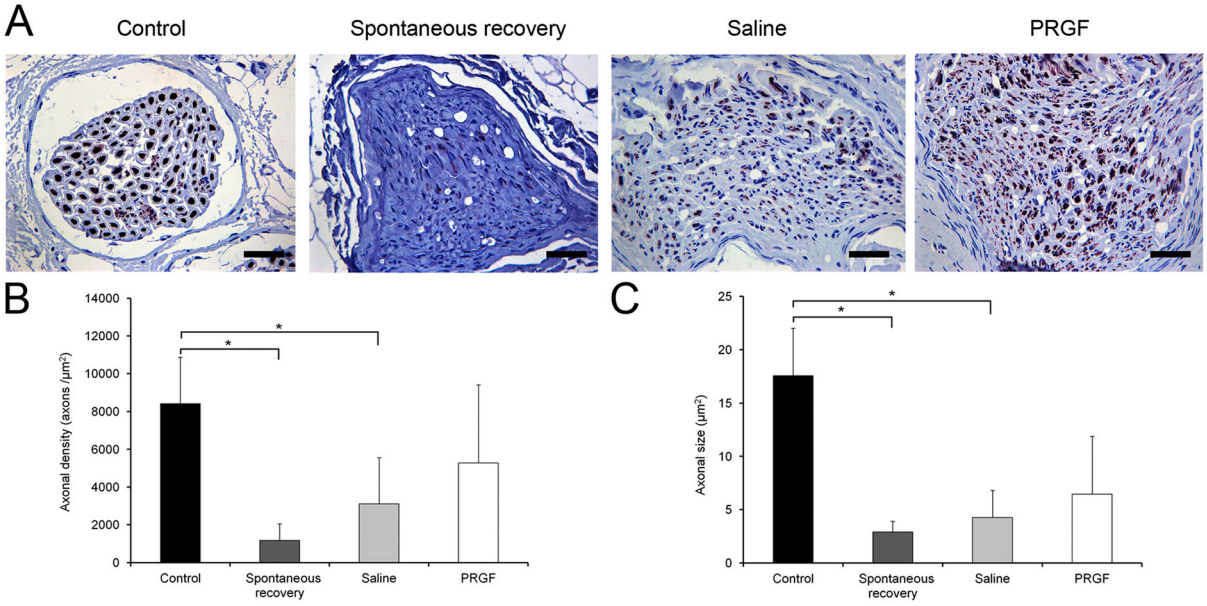

Figure 5. Nerve histological analysis. (A) Photomicrographs of cross-sections of peripheral nerve stained with neurofilament to demonstrate the presence of axons. Control group (contralateral non-injured) and injured groups (untreated, and infiltrated with saline and PRGF) are shown. Histomorphometric results for density of axons (B) and axonal size (C) are plotted; *$p < 0.05$; scale bars = 50 µm

DOI: 10.1002/term

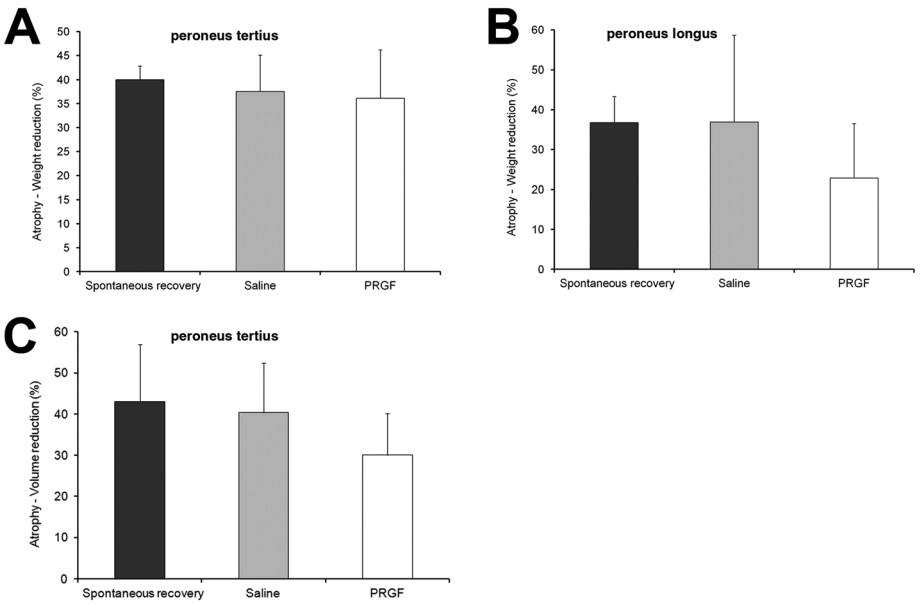

Figure 6. Muscle macroscopic atrophy evaluation. Percentage weight reduction of (A) peroneous tertius and (B) peroneus longus muscles with reference to weight of contralateral non-injured muscle. (C) Volume reduction of peroneous tertius muscle

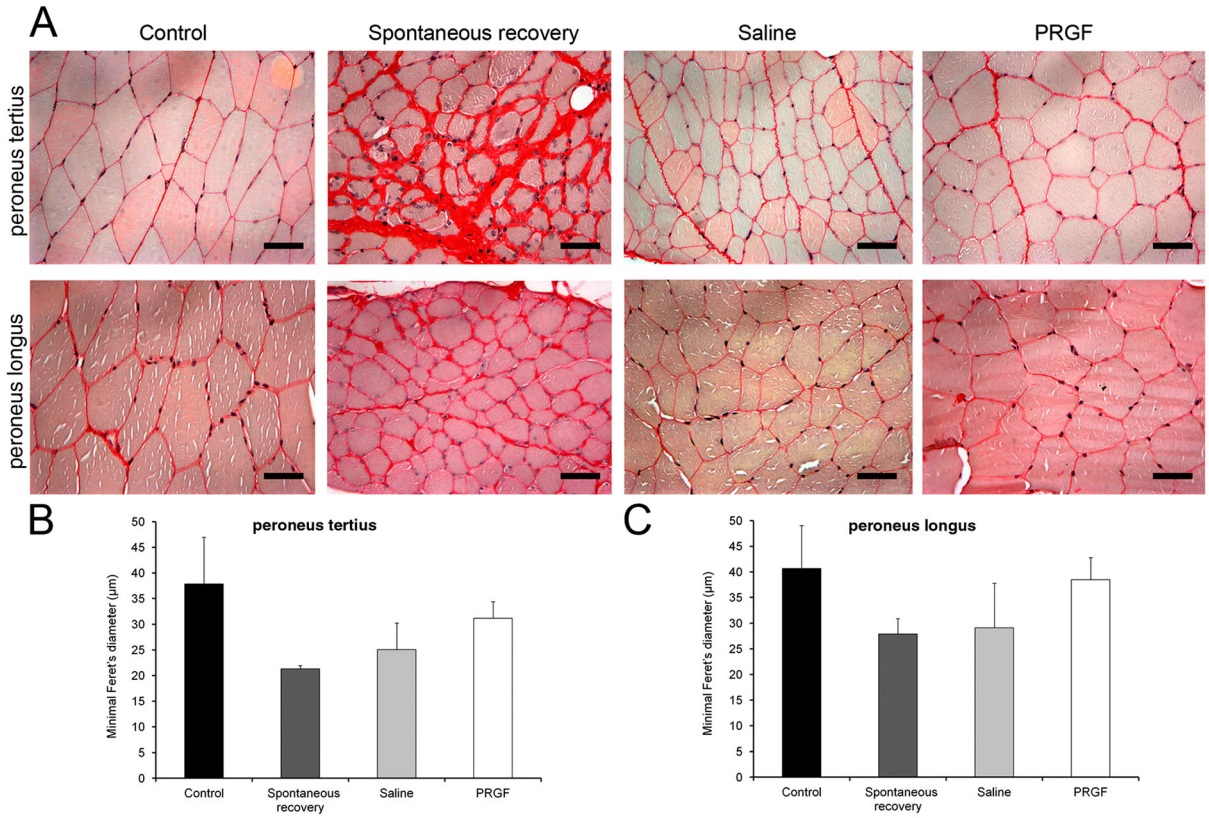

Figure 7. Muscle histological analysis. (A) Cross-sectional micrographs of target muscles stained with picrosirius red: control group (contralateral non-injured) and injured groups (untreated, and infiltrated with saline and PRGF) are shown. Histomorphometric results for minimal Feret's diameter for myofibre cross-sectional area of (B) peroneous tertius and (C) peroneus longus muscles; scale bars = 50 µm

for the attenuation of target muscle atrophy found in the PRGF group at post-intervention week 12.

To evaluate the motor recovery process of peripheral nerve injuries, there are several methods and electrophysiology and histomorphometry are among the most commonly accepted (Archibald *et al.*, 1991; Wang *et al.*, 2008; Zheng *et al.*, 2014). The early occurrence of CMAP in the PRGF group at week 8 is consistent with superior axonal density and larger axonal size, histomorphometric data which indicate a higher degree of myelination and

DOI: 10.1002/term

axonal maturity (Archibald *et al*., 1991; Sariguney *et al*., 2008; Wang *et al*., 2008) seen in the nerves of the PRGF group at post-injury week 12. In addition, this earlier presence of CMAP, whose amplitude is proportional to the number of motor axons that have established a connection with the target muscle, might account for the attenuation of the muscle atrophy shown by the PRGF group, which presented larger muscle fibres and lower muscle volume reduction than the SR and SI groups. Therefore, the treatment of acute nerve crush injuries with PRGF injections and scaffolds promotes and hastens axonal growth and thereby may dampen the target muscle atrophy (Ma *et al*., 2011; Sariguney *et al*., 2008; Schaakxs *et al*., 2013; Zheng *et al*., 2014). This finding is very encouraging since, in the case of humans and despite careful surgical nerve repair, target muscle atrophy is often a recovery burden that plays havoc with complete functional nerve regeneration.

There are several potential mechanisms by which PRGF injections and scaffolds, as they convey neurotrophic (NGF, BDGF, IGF-1, FGF, PDGF, VEGF) and neurotropic (fibrin and fibronectin) factors (Anitua *et al*., 2013, 2015), might promote and speed up axonal regeneration (Allodi *et al*., 2012). VEGF is the master switch of the angiogenic cascade and, in addition to promoting vascularization along the fibrin cable, which is critical for and precedes axon regeneration (Hoke *et al*., 2001), might act in concert with TGFβ to decrease inflammation and in so doing contribute to the generation of a trophic microenvironment that is conducive to the survival, proliferation and differentiation of Schwann cells (SCs), as well as the release of neurotrophic factors by SCs (Luo *et al*., 2012; Sulaiman and Gordon, 2002; Zheng *et al*., 2007). Other growth factors within the fibrin matrix that are gradually released from it are IGF-1, BDNF, NGF, PDGF (Anitua *et al*., 2015; Martino *et al*., 2013), and that, together with fibrin and fibronectin, have been shown to influence SC survival, proliferation and migration (Akassoglou *et al*., 2003; Cheng *et al*., 1999; Lee *et al*., 2003; Mohammadi *et al*., 2013; Ogata *et al*., 2006; Oya *et al*., 2002; Zheng *et al*., 2013) in addition to increasing myelination of the newly sprouted axons (Eccleston *et al*., 1993; Emel *et al*., 2011; Farrag *et al*., 2007; Oya *et al*., 2002). As a consequence, it is reasonable to speculate that neurotrophic and neurotropic factors within the PRGF (Anitua *et al*., 2013) might exert their synergistic action in a biphasic manner on the SC phenotypes, which are the masters and servers of the nerve regeneration process. At the onset of the repair process in the injured area, released of FGF, PDGF, IGF-1, NGF and BDGF from the fibrin matrix would induce a powerful SC proliferation (Akassoglou *et al*., 2002; Sakiyama-Elbert and Hubbell, 2000), whereas fibrin and fibronectin would simultaneously promote migration and homing while inhibiting the differentiation of proliferating SCs (Akassoglou *et al*., 2002; Chernousov and Carey, 2003). The leakage of fibrinogen deposited in the damaged nerve, and stemming from the disruption of the blood–nerve barrier and the fibrin of PRGF molecular intervention, would gradually be removed as a result of local activation of the tissue plasminogen activator/plasminogen system (Akassoglou *et al*., 2000; Anitua *et al*., 2015). This new SC microenvironment would give way to a non-proliferating, myelin-synthezising SC phenotype, thereby carrying out the remyelination of the newly sprouted axons (Akassoglou *et al*., 2002, 2003; Lee *et al*., 2003).

To the best of our knowledge, no one has injected injured nerve intraneurally and scaffolded it with an autologous PRP in a large animal model as an acute treatment for PNI. PRGF injections and scaffold might be considered an optimum scaffold for nerve repair, since they provide the injured site and severed nerve ends with a biodegradable scaffold via normal metabolic pathways, and which will in 1–3 weeks be removed (Akassoglou *et al*., 2002; Anitua *et al*., 2015). Its resorption modulates SC phenotypes (Akassoglou *et al*., 2002, 2003), serve as a mechanical support for cell homing and a guidance for regenerating axons (Chernousov and Carey, 2003) and conveys a plethora of neurotrophic and neurotropic factors (Anitua *et al*., 2015; Martino *et al*., 2013), with no antigenic and toxic reactions.

The improvement of SI group in some parameters compared to the SR group highlights the importance of a mechanical effect by opening the nerve crush injury and trying to restore the original tubular three-dimensional structure of the nerve. Maintaining an aligned extracellular matrix is essential for increasing peripheral nerve regeneration (Lundborg, 2004), but a simply mechanical stimulus (saline injection) is not enough, and PRGF infiltration and formation of scaffold is necessary to achieve a greater therapeutic effect.

It could be thought that any substance infiltration in nerve produces damage; however, the benefit is evident in our ovine crush nerve model. Overall, saline infiltration was used as a control in many animal studies. Thus, Strasberg *et al*. (1999) showed in a rat sciatic nerve model that nerves injected with normal saline had no evidence of damage or degeneration. More recently, Farber *et al*. (2013) observed no injury at the ultrastructural level (apart from the occasional injury caused by the needle) in the saline group of rats of a study demonstrating injury after local anaesthetic injections. However, severe damage was found after infiltrating the same volumes of anaesthetics.

There are several limitations to this study. The findings gathered in this research must be interpreted with caution, due to the small number of animals and inter-individual variability, thereby making it difficult to determine with confidence the therapeutic effect of the PRGF in this case, but knowing that studies on large mammals such as sheep are complex to carry out with a large number of animals (Angius *et al*., 2012). Since SCs play such a key role in nerve regeneration, it would have been more informative about repair timing to have their evaluation done, as well as performing the rest of the histological evaluations, together with different points of electrophysiological assessment, every 2 weeks. There remain some mechanistic and dosage aspects that must be elucidated,

DOI: 10.1002/term

and their implementation entails a complex research project, as PRGF therapy draws on the autologous biological system of growth factors and fibrin that exert a broad regulatory and pleiotropic function. There seems to be no specific protein as a discrete entity for each specific cellular function (Huang, 2004), but rather there are biological factors which, in a particular tissue environment and acting together, induce the expression of cell phenotypes with different behaviours.

Overall, the electrophysiological, histomorphometric and muscle evaluation data suggest that PRGF injections and scaffolds applied to acute peripheral nerve injuries hasten functional axon recovery and dampen target muscle atrophy in an ovine model.

Abbreviations and acronyms

BDNF, brain-derived neurotrophic factor; EGF, epidermal growth factor; CMAP, compound muscle action potential; CPN, common peroneal nerve; FGF, fibroblast growth factor; GFs, growth factors; HGF, hepatocyte growth factor; IGF-1, insulin-like growth factor-1; NGF, nerve growth factor; PDGF, platelet-derived growth factor; PNI, peripheral nerve injury; PRGF, plasma rich in growth factors; PRP, platelet-rich plasma; SC, Schwann cells; SI, saline injections; SR, spontaneous recovery; TGFβ, transforming growth factor-β; VEGF, vascular endothelial growth factor.

Conflicts of interest

E. Anitua is the scientific director and R. Prado and S. Padilla are scientists at BTI-Biotechnology Institute, the company that has developed the PRGF–Endoret technology.

Acknowledgements

The authors wish to thank Fernando Yangüela for support with ultrasound-guided injections. Ignacia Beltrán de Heredia, Roberto Pascual and Iñaki Diaz are acknowledged for their excellent collaboration and animal care. The authors also wish to thank Katti Perez de Heredia for the efficient collection and processing of the samples.

References

Akassoglou K, Akpinar P, Murray S *et al*. 2003; Fibrin is a regulator of Schwann cell migration after sciatic nerve injury in mice. *Neurosci Lett* **338**: 185–188.

Akassoglou K, Kombrinck KW, Degen JL *et al*. 2000; Tissue plasminogen activator-mediated fibrinolysis protects against axonal degeneration and demyelination after sciatic nerve injury. *J Cell Biol* **149**: 1157–1166.

Akassoglou K, Yu WM, Akpinar P *et al*. 2002; Fibrin inhibits peripheral nerve remyelination by regulating Schwann cell differentiation. *Neuron* **33**: 861–875.

Allodi I, Udina E, Navarro X. 2012; Specificity of peripheral nerve regeneration: interactions at the axon level. *Prog Neurobiol* **98**: 16–37.

Angius D, Wang H, Spinner RJ *et al*. 2012; A systematic review of animal models used to study nerve regeneration in tissue-engineered scaffolds. *Biomaterials* **33**: 8034–8039.

Anitua E, Pascual C, Perez-Gonzalez R *et al*. 2013; Intranasal delivery of plasma and platelet growth factors using PRGF–Endoret system enhances neurogenesis in a mouse model of Alzheimer's disease. *PLoS One* **8**: e73118.

Anitua E, Prado R, Sánchez M *et al*. 2012; Platelet-rich plasma: preparation and formulation. *Oper Tech Orthop* **22**: 25–32.

Anitua E, Sanchez M, Orive G. 2010; Potential of endogenous regenerative technology for *in situ* regenerative medicine. *Adv Drug Deliv Rev* **62**: 741–752.

Anitua E, Zalduendo MM, Prado R *et al*. 2015; Morphogen and proinflammatory cytokine release kinetics from PRGF–Endoret fibrin scaffolds: evaluation of the effect of leukocyte inclusion. *J Biomed Mater Res A* **103**: 1011–1020.

Archibald SJ, Krarup C, Shefner J *et al*. 1991; A collagen-based nerve guide conduit for peripheral nerve repair: an electrophysiological study of nerve regeneration in rodents and nonhuman primates. *J Comp Neurol* **306**: 685–696.

Borselli C, Storrie H, Benesch-Lee F *et al*. 2010; Functional muscle regeneration with combined delivery of angiogenesis and myogenesis factors. *Proc Natl Acad Sci USA* **107**: 3287–3292.

Boswell SG, Schnabel LV, Mohammed HO *et al*. 2014; Increasing platelet concentrations in leukocyte-reduced platelet-rich plasma decrease collagen gene synthesis in tendons. *Am J Sports Med* **42**: 42–49.

Briguet A, Courdier-Fruh I, Foster M *et al*. 2004; Histological parameters for the quantitative assessment of muscular dystrophy in the mdx-mouse. *Neuromuscul Disord* **14**: 675–682.

Cheng HL, Feldman EL. 1997; Insulin-like growth factor-I (IGF-I) and IGF binding protein-5 in Schwann cell differentiation. *J Cell Physiol* **171**: 161–167.

Cheng HL, Russell JW, Feldman EL. 1999; IGF-I promotes peripheral nervous system myelination. *Ann NY Acad Sci* **883**: 124–130.

Chernousov MA, Carey DJ. 2003; $\alpha V\beta 8$ integrin is a Schwann cell receptor for fibrin. *Exp Cell Res* **291**: 514–524.

Currie J, Ramsbottom R, Ludlow H *et al*. 2009; Cardio-respiratory fitness, habitual physical activity and serum brain derived neurotrophic factor (BDNF) in men and women. *Neurosci Lett* **451**: 152–155.

Daly WT, Knight AM, Wang H *et al*. 2013; Comparison and characterization of multiple biomaterial conduits for peripheral nerve repair. *Biomaterials* **34**: 8630–8639.

de Boer R, Borntraeger A, Knight AM *et al*. 2012; Short- and long-term peripheral nerve regeneration using a poly-lactic-co-glycolic-acid scaffold containing nerve growth factor and glial cell line-derived neurotrophic factor releasing microspheres. *J Biomed Mater Res A* **100**: 2139–2146.

Deumens R, Bozkurt A, Meek MF *et al*. 2010; Repairing injured peripheral nerves: bridging the gap. *Prog Neurobiol* **92**: 245–276.

Eccleston PA, Funa K, Heldin CH. 1993; Expression of platelet-derived growth factor (PDGF) and PDGFα- and β-receptors in the peripheral nervous system: an analysis of sciatic nerve and dorsal root ganglia. *Dev Biol* **155**: 459–470.

Emel E, Ergun SS, Kotan D *et al*. 2011; Effects of insulin-like growth factor-I and platelet-rich plasma on sciatic nerve crush injury in a rat model. *J Neurosurg* **114**: 522–528.

Farber SJ, Saheb-Al-Zamani M, Zieske L *et al*. 2013; Peripheral nerve injury after local anesthetic injection. *Anesth Analg* **117**: 731–739.

Farrag TY, Lehar M, Verhaegen P *et al*. 2007; Effect of platelet rich plasma and fibrin sealant on facial nerve regeneration in a rat model. *Laryngoscope* **117**: 157–165.

Hobson MI, Green CJ, Terenghi G. 2000; VEGF enhances intraneural angiogenesis and improves nerve regeneration after axotomy. *J Anat* **197 Pt 4**: 591–605.

Höke A. 2006; Mechanisms of disease: what factors limit the success of peripheral nerve regeneration in humans? *Nat Clin Pract Neurol* **2**: 448–454.

Hoke A, Sun HS, Gordon T *et al*. 2001; Do denervated peripheral nerve trunks become ischemic? The impact of chronic denervation on vasa nervorum. *Exp Neurol* **172**: 398–406.

Huang S. 2004; Back to the biology in systems biology: what can we learn from biomolecular networks? *Brief Funct Genom Proteom* **2**: 279–297.

Ikeda M, Uemura T, Takamatsu K *et al*. 2014; Acceleration of peripheral nerve regeneration using nerve conduits in combination with induced pluripotent stem cell technology and a basic fibroblast growth factor drug delivery system. *J Biomed Mater Res A* **102**: 1370–1378.

Jungnickel J, Haase K, Konitzer J *et al*. 2006; Faster nerve regeneration after sciatic nerve injury in mice over-expressing basic fibroblast growth factor. *J Neurobiol* **66**: 940–948.

Kuffler DP. 2014; An assessment of current techniques for inducing axon regeneration and neurological recovery following peripheral nerve trauma. *Prog Neurobiol* **116**: 1–12.

Lee AC, Yu VM, Lowe JB III *et al*. 2003; Controlled release of nerve growth factor enhances sciatic nerve regeneration. *Exp Neurol* **184**: 295–303.

Lundborg G. 2004; Acute nerve compression. In *Nerve Injury and Repair*, 2nd edn, Chapter 4, Lundborg G (ed.). Churchill Livingstone: Philadelphia, PA: 49–71.

Luo H, Zhang Y, Zhang Z *et al*. 2012; The protection of MSCs from apoptosis in nerve regeneration by TGFβ1 through reducing inflammation and promoting VEGF-dependent angiogenesis. *Biomaterials* **33**: 4277–4287.

Ma CH, Omura T, Cobos EJ *et al*. 2011; Accelerating axonal growth promotes motor recovery after peripheral nerve injury in mice. *J Clin Invest* **121**: 4332–4347.

Martino MM, Briquez PS, Ranga A *et al*. 2013; Heparin-binding domain of fibrin (ogen) binds growth factors and promotes tissue repair when incorporated within a synthetic matrix. *Proc Natl Acad Sci U S A* **110**: 4563–4568.

Mohammadi R, Esmaeil-Sani Z, Amini K. 2013; Effect of local administration of insulin-like growth factor I combined with inside-out artery graft on peripheral nerve regeneration. *Injury* **44**: 1295–1301.

Nurden AT, Nurden P, Sanchez M *et al*. 2008; Platelets and wound healing. *Front Biosci* **13**: 3532–3548.

Ogata T, Yamamoto S, Nakamura K *et al*. 2006; Signaling axis in Schwann cell proliferation and differentiation. *Mol Neurobiol* **33**: 51–62.

Oya T, Zhao YL, Takagawa K *et al*. 2002; Platelet-derived growth factor-β expression induced after rat peripheral nerve injuries. *Glia* **38**: 303–312.

Rodríguez FJ, Valero-Cabré A, Navarro X. 2004; Regeneration and functional recovery following peripheral nerve injury. *Drug Discov Today Dis Models* **1**: 177–185.

Rosner BI, Hang T, Tranquillo RT. 2005; Schwann cell behavior in three-dimensional collagen gels: evidence for differential mechano-transduction and the influence of TGF-β1 in morphological polarization and differentiation. *Exp Neurol* **195**: 81–91.

Sakiyama-Elbert SE, Hubbell JA. 2000; Controlled release of nerve growth factor from a heparin-containing fibrin-based cell ingrowth matrix. *J Control Release* **69**: 149–158.

Sanchez M, Yoshioka T, Ortega M *et al*. 2014; Ultrasound-guided platelet-rich plasma injections for the treatment of common peroneal nerve palsy associated with multiple ligament injuries of the knee. *Knee Surg Sports Traumatol Arthrosc* **22**: 1084–1089.

Sariguney Y, Yavuzer R, Elmas C *et al*. 2008; Effect of platelet-rich plasma on peripheral nerve regeneration. *J Reconstr Microsurg* **24**: 159–167.

Schaakxs D, Kalbermatten DF, Raffoul W *et al*. 2013; Regenerative cell injection in denervated muscle reduces atrophy and enhances recovery following nerve repair. *Muscle Nerve* **47**: 691–701.

Strasberg JE, Atchabahian A, Strasberg SR *et al*. 1999; Peripheral nerve injection injury with antiemetic agents. *J Neurotrauma* **16**: 99–107.

Sulaiman OA, Gordon T. 2002; Transforming growth factor-β and forskolin attenuate the adverse effects of long-term Schwann cell denervation on peripheral nerve regeneration *in vivo*. *Glia* **37**: 206–218.

Takeuchi M, Kamei N, Shinomiya R *et al*. 2012; Human platelet-rich plasma promotes axon growth in brain–spinal cord coculture. *Neuroreport* **23**: 712–716.

Tang S, Zhu J, Xu Y *et al*. 2013; The effects of gradients of nerve growth factor immobilized PCLA scaffolds on neurite outgrowth *in vitro* and peripheral nerve regeneration in rats. *Biomaterials* **34**: 7086–7096.

Wang H, Sorenson EJ, Spinner RJ *et al*. 2008; Electrophysiologic findings and grip strength after nerve injuries in the rat forelimb. *Muscle Nerve* **38**: 1254–1265.

Wood MD, Moore AM, Hunter DA *et al*. 2009; Affinity-based release of glial-derived neurotrophic factor from fibrin matrices enhances sciatic nerve regeneration. *Acta Biomater* **5**: 959–968.

Wu CC, Wu YN, Ho HO *et al*. 2012; The neuroprotective effect of platelet-rich plasma on erectile function in bilateral cavernous nerve injury rat model. *J Sex Med* **9**: 2838–2848.

Ye F, Li H, Qiao G *et al*. 2012; Platelet-rich plasma gel in combination with Schwann cells for repair of sciatic nerve injury. *Neural Regen Res* **7**: 2286–2292.

Yin Q, Kemp GJ, Yu LG *et al*. 2001; Neurotrophin-4 delivered by fibrin glue promotes peripheral nerve regeneration. *Muscle Nerve* **24**: 345–351.

Zheng C, Zhu Q, Liu X *et al*. 2013; Effect of platelet-rich plasma (PRP) concentration on proliferation, neurotrophic function and migration of Schwann cells *in vitro*. *J Tissue Eng Regen Med*. doi: 10.1002/term.1756

Zheng C, Zhu Q, Liu X *et al*. 2014; Improved peripheral nerve regeneration using acellular nerve allografts loaded with platelet-rich plasma. *Tissue Eng A* **20**: 3228–3240.

Zheng H, Fu G, Dai T *et al*. 2007; Migration of endothelial progenitor cells mediated by stromal cell-derived factor-1α/CXCR4 via PI3K/Akt/eNOS signal transduction pathway. *J Cardiovasc Pharmacol* **50**: 274–280.

Supporting information on the internet

The following supporting information may be found in the online version of this article:

Table S1. Characteristics of the experimental groups
Video S1. Ultrasound-guided infiltration